Toward data-domain Waveform Inversion of reflected waves

Romain Brossier[*], *Stéphane Operto*[†], *Jean Virieux*[*]
[*]*ISTerre, Univ. Joseph Fourier Grenoble,* [†]*Géoazur, Univ. Nice Sophia-Antipolis - CNRS*

SUMMARY

Full Waveform Inversion (FWI) is becoming a powerful tool for quantitative seismic imaging from wide-azimuth seismic data. The method is today mainly used as a high-resolution tomography of the Earth zones sampled by both reflected and diving events. However, the classical formulation of FWI prevents the reconstruction of the low part of the wavenumber spectrum of the velocity model from reflection-only data. The use of reflections in waveform inversion is a crucial challenge for deep imaging. This study, through a simple canonical example, first analyses the issue of classical waveform inversion when applied on reflection data. Then we show that, if a prior knowledge of the reflectivity is available, reflected waves can be exploited to retrieve the long wavelengths of the velocity, in particular when we use appropriate misfit measurement as the cross-correlation that overcome cycle-skipping issues, and inversion domain as the pseudo-depth domain that preserves the invariant property of zero-offset time.

INTRODUCTION

Full Waveform Inversion (FWI) is becoming a powerful technique to reconstruct high resolution velocity models (and other parameters) of the subsurface using theoretically the full information contained in seismic data (Lailly, 1983; Tarantola, 1984; Pratt and Worthington, 1990; Virieux and Operto, 2009). FWI relies on the diffraction tomography principle (Devaney, 1982), and the imaged spatial frequency $\vec{\mathbf{k}}$ is related to the wavelength and diffraction angle θ through the relation

$$\vec{\mathbf{k}} = \frac{2\omega}{c_0}\cos\left(\frac{\theta}{2}\right)\vec{\mathbf{n}}, \qquad (1)$$

where ω is the angular frequency, c_0 the local wave speed and $\vec{\mathbf{n}}$ the direction provided by the sum of slowness vectors from the source and receiver at the diffractor point. When considering only reflected waves and limited offset ranges, the diffraction angle θ remains small and only the high part of the spatial frequency spectrum can be retrieved. This limited bandwidth reconstruction leads to the well known scale separation between the velocity macro model and the reflectivity (Jannane et al., 1989). This scale separation prevents classical FWI to retrieve the long wavelengths of the velocity field from reflection-only data. This leads to two different behaviors of classical FWI when applied on surface data (Plessix, 2012) : (1) broaband velocity model building in the shallow part from both transmitted and reflected events. (2) non-linear migration of short-spread reflections in the deep part of the subsurface, assuming that the low part of the velocity spectrum is sufficiently accurate to avoid cycle-skipping issues.

In order to establish better-posed problems to retrieve the long wavelengths of the velocity from reflected waves, several approaches have been proposed based on image-domain optimization as the Differential Semblance Optimization (Symes and Carazzone, 1991) or Wave-Equation Migration Velocity Analysis (Sava and Biondi, 2004). These approaches attempt to maximize focusing or coherency of energy in the image-domain instead of minimizing data residuals in the data domain as FWI does. The measure of focusing relies on extended-domain imaging conditions computed during migration, through time shift or subsurface offset shift (Sava and Fomel, 2006). The main issue of such approaches is the cost of the migration at each velocity update step and the additional computational cost of the extended-domain imaging condition, that prevents the direct extension to 3D with two-way wave-equation modeling. Recent applications of such image-domain and mixed image/data-domain approaches have shown promising results (Yang and Sava, 2011; Almomin and Biondi, 2012; Biondi and Almomin, 2012; Sun and Symes, 2012), although they remain limited to 2D geometries and rely on some approximations to keep computer cost affordable. Data-domain approaches have also been proposed to mitigate non-linearities of classical least-square FWI formulation, as the Migration Based Traveltime Tomography (MBTT) (Chavent et al., 1994; Xu et al., 2012). This method relies on a difference-based data-fitting approach and requires also a migration step at each iteration to estimate the reflectivity field that produces the diffracted field.

In this study, we limit ourselves to data-domain approaches without migration step at each iteration, which should dramatically limit the computational cost when moving to 3D data. We consider here a simple configuration to understand the intrinsic limits of classical FWI when applied on reflection-only data, and we explore some alternative waveform inversion formulation, to overcome these limits and to reconstruct the low-frequency part of the velocity spectrum.

THEORY

The classical formulation of FWI attempts to minimize the difference between observed and computed data, in the L_2 sense through the misfit function

$$C_{diff} = \sum_h \sum_t \frac{1}{2}\left(d_{cal}(t,h) - d_{obs}(t,h)\right)^2, \qquad (2)$$

where $d_{cal}(t,h)$ and $d_{obs}(t,h)$ are respectively the computed and observed data, at time t and offset h. An implicit sum over sources is also contained in equation (2). The derivative of the misfit function with respect to the velocity gives

$$G_{diff} = \sum_h \sum_t \frac{\partial d_{cal}(t,h)}{\partial m}\Delta d(t,h), \qquad (3)$$

where $\partial d_{cal}(t,h)/\partial m$ is the Fréchet derivative of data recorded at time t and position h. In practice, these derivatives are

DOI http://dx.doi.org/10.1190/segam2013-0897.1

never computed and the gradient is directly computed with the adjoint-state method (Plessix, 2006).

van Leeuwen and Mulder (2008) introduced a weighted time cross-correlation misfit function, defined as

$$C_{XcorrN} = \sum_h \sum_\tau \frac{1}{2} \Big(P(\tau) XcorrN(\tau,h) \Big)^2, \qquad (4)$$

where $P(\tau)$ is a weighting/penalization function and τ is the time-lag of the normalized cross-correlation function $XcorrN(\tau,h)$ defined as :

$$XcorrN(\tau,h) = \frac{\sum_t d_{cal}(t,h) d_{obs}(t+\tau,h)}{||d_{cal}(h)||||d_{obs}(h)||}. \qquad (5)$$

Note that the proposed misfit function is not the zero-lag-only cross-correlation of Routh et al. (2011). Therefore, the misfit function (4) is able to handle time (phase) delay larger that half a period without ambiguity.

Deriving the misfit function with respect to the velocity gives the gradient of the time normalized cross-correlation

$$\frac{\partial C_{XcorrN}}{\partial m_i} = \sum_h \sum_t \frac{\partial d_{cal}(t,h)}{\partial m_i}^t \sum_\tau P(\tau)^2 XcorrN(\tau,h) \left(\frac{d_{obs}(\tau+t,h)}{||d_{cal}(h)||||d_{obs}(h)||} - \frac{Xcor(\tau,h) d_{cal}(t,h)}{||d_{cal}(h)||^3 ||d_{obs}(h)||} \right). \qquad (6)$$

Note that this gradient can be computed at the same computational cost than the classical gradient (equation 3). The only modification is the source term of the adjoint-state equation (Tromp et al., 2005).

In the following applications, these misfit function and gradient formulations are used in a 2D acoustic inversion algorithm, in which optimization relies on a L-BFGS-B scheme for both Hessian estimation and line-search satisfying Wolfe's conditions (Byrd et al., 1995).

RESULTS

We consider a reflection geometry in a square box of size 500 m $\times$ 500 m. The true model is formed by an homogeneous velocity background of 1500m/s and an homogeneous density background of 1500 kg/m^3, in which a density reflector is set at 340 m in depth with a value of 2500 kg/m^3 (Figure 1(a-b)). Twenty-one explosive sources are located with a 25-m space-step at the surface from 0 m to 500 m and 201 receivers are located with a 5-m space-step at the surface. A Ricker wavelet of central frequency 26 Hz is used. The shot gathers contain the direct wave and the reflected wave, this later being generated by the impedance contrast (Figure 1c). The direct wave is muted and only the reflected wave is considered in the inversion (Figure 1(d)). In the following of this study, the starting velocity model is homogeneous with an overestimated velocity of 1800 m/s.

No knowledge of reflector

In a first test, an homogeneous density model is considered, implying that no reflection is generated by the starting model. In such a case, only the difference-based inversion can be used, as the cross-correlation misfit is zero in the starting model

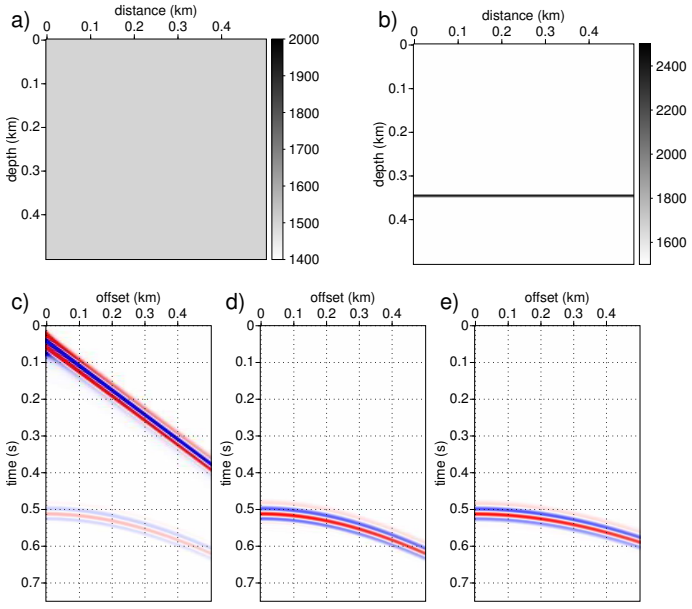

Figure 1: True Velocity (a) and density (b) models. (c) Shot gather for the first source. (d) Data used during FWI after mute of the direct wave. (e) Reflected wave generated by the initial model with the density contrast and the wrong velocity.

when the direct arrival is muted. Figure 2(a)-(b) shows that inversion attempts to create a velocity perturbation that mimics the impedance contrast to generate the reflection, but at the wrong depth as the short spread reflection are unable to update the large wavelengths of the velocity model. This test shows the classical failure of FWI with reflected waves when the velocity model is not accurate enough.

Knowledge of reflectivity

In the following tests, a density model containing the true impedance contrast is used to generate a reflected wave. This density model is built from the zero-offset traveltime in the starting velocity of 1800 m/s, implying that the reflector is positioned at a depth of 410 m instead of 340 m. This density model could have been created from an impedance analysis in the starting velocity model. The first shot-gather computed in this starting model (Figure 1(e)) shows the correct arrival time at zero-offset but the wrong move-out due to the erroneous velocity above the reflector.

A key change relative to the previous test (Figure 2(a)-(b)) is the presence of the reflector in the starting model. As the reflector is already in the starting model, the sensitivity kernel of the FWI is completely different (Figure 2(c)-(d)). Without the knowledge of reflectivity, the kernel exhibits a high sensitivity at all the spatial positions corresponding to a constructive correlation of the incident field and the backpropagated field of the reflected wave in order to generate a discontinuity that generates the reflection in the modeled data. With the knowledge of reflectivity, the kernel behaves as a transmission kernel with a sensitivity along the two wavepaths connecting the source and the receiver to the reflector. These transmission kernels should thus be able to update the long wavelengths of

DOI http://dx.doi.org/10.1190/segam2013-0897.1

the velocity from the large diffraction angles. These kernels highlight how a prior knowledge on the reflectivity in the starting model allows for the reconstruction of the low part of the wavenumber spectrum from the transmitted wavepaths of the reflected waves.

Figure 3 shows the inversion results for the two misfit functions when a prior knowledge of the reflectivity is used (here through density). Note, that this density model is consistent in term of zero-offset time in the starting velocity model, but as soon as inversion updates the velocity over iterations, one would need to update the density model accordingly. Here, we do not update the density model. Due to cycle-skipping issues, the difference misfit function is unable to correct properly the velocity model. The cross-correlation is slightly better in terms of data fit, but the velocity model is still inaccurate as the fixed density model over iterations prevents the convergence toward the true model.

Reflectivity knowledge in the depth/pseudo-time domain ? The previous test is suffering from the constant density model over the iterations. One solution would be to estimate the reflectivity from impedance analysis or migration at each iteration of velocity update (Chavent et al., 1994; Xu et al., 2012). Another solution, which is chosen here to avoid the migration cost, is to work in an alternative domain. The vertical travel-time domain, also called pseudo-time by Plessix et al. (2012), was proposed by Alkhalifah et al. (2001) for seismic processing in anisotropic media and Ma and Alkhalifah (2011) formulate a modeling technique directly in this alternative domain. In the pseudo-time domain, we consider a variable change that transforms the local depth (z) coordinate in a local zero-offset vertical travel-time (τ) coordinate. Considering the local depth-domain velocity $v(z)$, the vertical travel-time is defined as

$$\tau = \int_0^z \frac{dz'}{v(z')}. \tag{7}$$

Conversely, the expression of the depth z as a function of the local pseudo-depth domain velocity $\tilde{v}(\tau)$ is given by

$$z = \int_0^\tau \tilde{v}(\tau')d\tau'. \tag{8}$$

Plessix et al. (2012) showed that we can avoid to formulate the full problem in the τ domain and still use standard depth domain modeling and inversion tools. The variable change is applied after the gradient computation using a chain rule such that the optimization is performed in the τ domain:

$$\frac{\partial C}{\partial \tilde{v}(\tau_i)} = \frac{\partial C}{\partial v(z_i)} - \int_{z_i}^{z_{max}} \frac{1}{v(z')}\frac{\partial v(z)}{\partial z}\frac{\partial C}{\partial v(z)}dz, \tag{9}$$

where

$$z_i = \int_0^{\tau_i} \tilde{v}(\tau')d\tau'. \tag{10}$$

leading to a relatively simple modification of existing inversion tool to perform FWI in the vertical travel-time domain. Landa et al. (1989); Snieder et al. (1989) also used the similar idea of using invariant properties of the zero-offset travel time.

Figure 4 shows the result of inversion in the vertical travel-time domain τ. Note that the results are plotted in the depth domain, but the inversion is performed in the τ domain. In this case, the difference misfit does not give robust result as convergence is hampered by cycle skipping at intermediate and large offsets due to the wrong move-out of the reflection computed in the starting model. In contrast, the time cross-correlation misfit inversion gives accurate result above the reflector, decreasing the velocity value toward 1500 m/s. As the density model is kept unchanged in the vertical travel-time domain, it is updated in the depth domain according to the velocity change: the reflector position is shifted up to 340 m depth in the depth domain. Please, note that, even in the pseudo-time domain, a robust error measure is required. Indeed, difference-based misfit is unable to succeed if the starting velocity is too erroneous, leading here to wrong move-out even if vertical time at zero-offset is correct. The same problem should occur if the inversion would be performed in the depth domain and reflectivity estimated at each iteration as done by Xu et al. (2012).

DISCUSSION AND CONCLUSIONS

We investigated alternative misfit measurement and domain of inversion for velocity model building from reflection data and wave-equation-based modeling.

The simple test first shows that a prior knowledge of reflectivity is necessary for the inversion to update the low part of the velocity spectrum from the downgoing and upgoing transmitted paths of reflected waves. Second, this knowledge should be combined with both a robust measure of data error, as the weighted cross-correlation, and an appropriate inversion domain, as the pseudo-time domain to prevent cycle skipping and exploit seismic invariant such as zero-offset traveltime. This combination allows for a robust exploitation of the information carried out by reflected waves to retrieve the low-part of the velocity wavenumber spectrum from their transmission regime.

It is well known that cross-correlation function suffers from cross-talks when applied on multi-arrival data. The cross-correlation should therefore be applied on appropriate domains where arrivals can be separeted or be applied locally (Hale, 2009). In order to keep computer cost low, data-domain separation could involves hyperbolic and/or non-hyperbolic move-out corrections, and slant-stack and/or double slant-stack on source and receiver sides (double beamforming). Alternative error measurement as dynamic warping could also be investigated, as it shows to provided robust results on multi-arrival seismic data (Hale, 2012). Of course, one could pay the price of migration to separate the data directly in the image domain, and link this study with image-oriented approaches.

ACKNOWLEDGEMENTS

This work was partially performed using the computing facilities of the SCCI department of CIMENT (Université Joseph Fourier, Grenoble). This work is partialy supported by the SEISCOPE consortium (*http://seiscope.oca.eu*), which is sponsored by BP, CGGVeritas, ENI, EXXON-Mobil, PETROBRAS, SAUDI ARAMCO, SHELL, STATOIL and TOTAL. The authors would like to thank L. Métivier (LJK, Univ. Grenoble - CNRS) and R.E. Plessix (SHELL) for fruitful discussions.

DOI http://dx.doi.org/10.1190/segam2013-0897.1

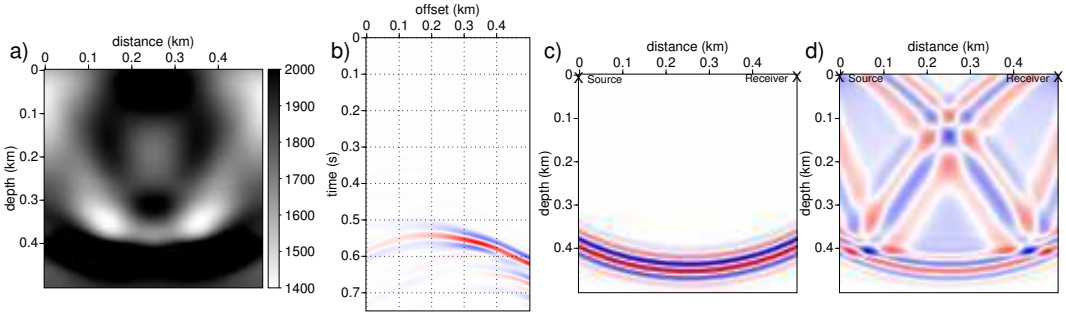

Figure 2: (a) FWI velocity model and (b) corresponding shot gather for the first source, inferred from the 1800 m/s starting velocity model and the homogeneous density model, using the difference-based misfit function. (c-d) Sensitivity kernels for the first source (x=0m) and the last receiver (x=500m) for (c) the homogeneous density and (d) the realistic density model containing the reflector at 410 m in depth.

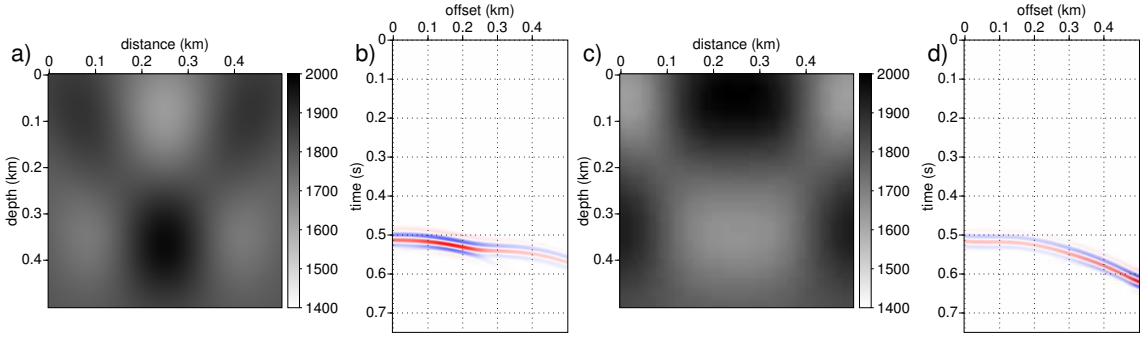

Figure 3: FWI velocity models and associated data for the first source, imaged from the 1800 m/s starting model and the density model containing a reflector at 410 m depth, using the difference-based misfit function (a-b) and time cross-correlation misfit function (c-d) in the depth domain.

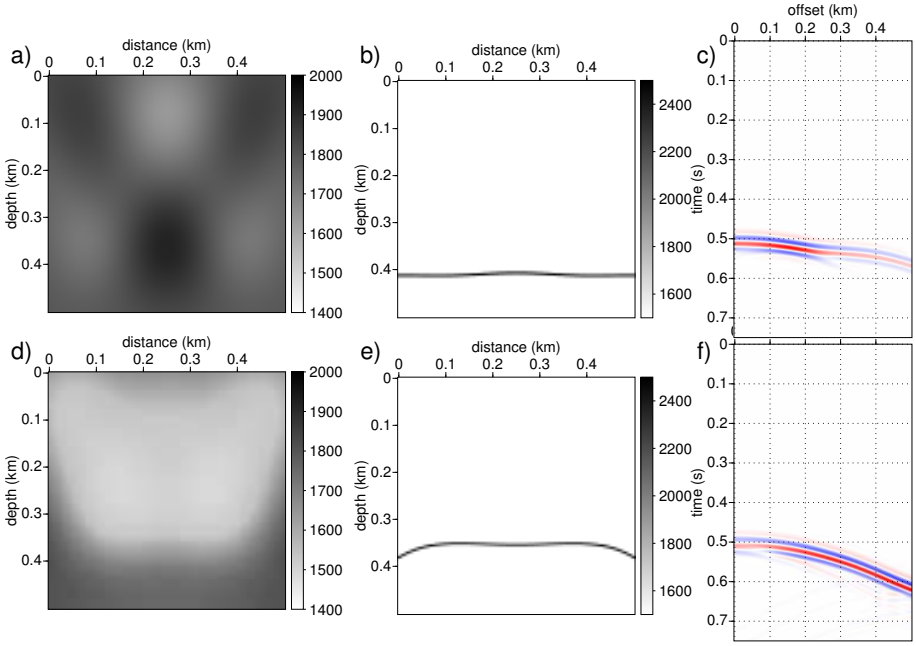

Figure 4: Velocity (a, d) and density (b, e) models, and associated data for the first source (c, f), imaged from the 1800 m/s starting model and the density model containing a reflector at 410 m depth, using the difference-based misfit function (a-c) and time cross-correlation misfit function (d-f) in the vertical time domain.

DOI http://dx.doi.org/10.1190/segam2013-0897.1

http://dx.doi.org/10.1190/segam2013-0897.1

EDITED REFERENCES

Note: This reference list is a copy-edited version of the reference list submitted by the author. Reference lists for the 2013 Annual International Meeting, SEG, Expanded Abstracts, have been copy edited so that references provided with the online metadata for each paper will achieve a high degree of linking to cited sources that appear on the Web.

REFERENCES

Alkhalifah, T., S. Fomel, and B. Biondi, 2001, The space-time domain: theory and modelling for anisotropic media : Geophysical Journal International, **144**, 105–113, http://dx.doi.org/10.1046/j.1365-246x.2001.00300.x.

Almomin, A., and B. Biondi, 2012, Tomographic full waveform inversion: Practical and computationally feasible approach: 82nd Annual International Meeting, SEG, Expanded Abstracts, http://dx.doi.org/10.1190/segam2012-0976.1.

Biondi, B., and A. Almomin, 2012, Tomographic full waveform inversion (TFWI) by combining full waveform inversion with wave-equation migration velocity analysis : 82nd Annual International Meeting, SEG, Expanded Abstracts, http://dx.doi.org/10.1190/segam2012-0275.1.

Byrd, R., P. Lu, J. Nocedal, and C. Zhu, 1995, A limited memory algorithm for bound constrained optimization: SIAM Journal on Scientific and Statistical Computing, **16**, 1190–1208, http://dx.doi.org/10.1137/0916069.

Chavent, G., F. Clément, and S. Gómez, 1994, Automatic determination of velocities via migration-based traveltime waveform inversion: A synthetic data example : 74th Annual International Meeting, SEG, Expanded Abstracts,1179–1182, http://dx.doi.org/10.1190/1.1822731.

Devaney, A. J., 1982, A filtered backpropagation algorithm for diffraction tomography: Ultrasonic Imaging, **4**, 336–350.

Hale, D., 2009, A method for estimating apparent displacement vectors from time-lapse seismic images: Geophysics, **74**, no. 5, V99–V107, http://dx.doi.org/10.1190/1.3184015.

Hale, D., 2012, Dynamic warping of seismic images: CWP Report 723.

Jannane, M., W. Beydoun, E. Crase, D. Cao, Z. Koren, E. Landa, M. Mendes, A. Pica, M. Noble, G. Roeth, S. Singh, R. Snieder, A. Tarantola, D. Trezeguet, and M. Xie, 1989, Wavelengths of Earth structures that can be resolved from seismic reflection data : Geophysics, **54**, 906–910, http://dx.doi.org/10.1190/1.1442719.

Landa, E., W. Beydoun, and A. Tarantola, 1989, Reference velocity model estimation from prestack waveforms: Coherency optimization by simulated annealing: Geophysics, **54**, 984–990, http://dx.doi.org/10.1190/1.1442741.

Lailly, P., 1983, The seismic inverse problem as a sequence of before stack migrations: Conference on Inverse Scattering, Theory and Application, SIAM, Philadelphia, Expanded Abstracts, 206–220.

Ma, X., and T. Alkhalifah, 2011, Wavefield extrapolation in the pseudo-depth domain: 73rd Conference & Exhibition, EAGE, Extended Abstracts, A014.

Plessix, R., P. Milcik, C. Corcoran, H. Kuehl, and K. Matson, 2012, Full waveform inversion with a pseudotime approach: 74th Conference & Exhibition, EAGE, Extended Abstracts, W012.

DOI http://dx.doi.org/10.1190/segam2013-0897.1

Plessix, R. E., 2006, A review of the adjoint-state method for computing the gradient of a functional with geophysical applications: Geophysical Journal International, **167**, 495–503, http://dx.doi.org/10.1111/j.1365-246X.2006.02978.x.

———, 2012, Waveform inversion overview: Where are we? And what are the challenges?: 74th Conference and Exhibition, EAGE, Extended Abstracts, 59982.

Pratt, R. G., and M. H. Worthington, 1990, Inverse theory applied to multi-source cross-hole tomography. Part I: acoustic wave-equation method: Geophysical Prospecting, **38**, 287–310, http://dx.doi.org/10.1111/j.1365-2478.1990.tb01846.x.

Routh, P., J. Krebs, S. Lazaratos, A. Baumstein, S. Lee, Y. H. Cha, I. Chikichev, N. Downey, D. Hinkley, and J. Anderson, 2011, Encoded simultaneous source full-wavefield inversion for spectrally shaped marine streamer data: 81st Annual International Meeting, SEG, Expanded Abstracts, 2433–2438, http://dx.doi.org/10.1190/1.3627697.

Sava, P., and B. Biondi, 2004, Wave-equation migration velocity analysis: I. Theory: Geophysical Prospecting, **52**, 593–606, http://dx.doi.org/10.1111/j.1365-2478.2004.00447.x.

Sava, P., and S. Fomel, 2006, Time-shift imaging condition in seismic migration: Geophysics, **71**, no. 6, S209–S217, http://dx.doi.org/10.1190/1.2338824.

Snieder, R., M. Y. Xie, A. Pica, and A. Tarantola, 1989, Retrieving both the impedance contrast and background velocity: a global strategy for the seismic reflection problem: Geophysics, **54**, 991–1000, http://dx.doi.org/10.1190/1.1442742.

Sun, D., and W. W. Symes, 2012, Waveform inversion via nonlinear differential semblance optimization: 82nd Annual International Meeting, SEG, Expanded Abstracts, http://dx.doi.org/10.1190/segam2012-1190.1.

Symes, W., and J. J. Carazzone, 1991, Velocity inversion by differential semblance optimization: Geophysics, **56**, 654–663, http://dx.doi.org/10.1190/1.1443082.

Tarantola, A., 1984, Inversion of seismic reflection data in the acoustic approximation: Geophysics, **49**, 1259–1266, http://dx.doi.org/10.1190/1.1441754.

Tromp, J., C. Tape, and Q. Liu, 2005, Seismic tomography, adjoint methods, time reversal and banana-doughnut kernels: Geophysical Journal International, **160**, 195–216, http://dx.doi.org/10.1111/j.1365-246X.2004.02453.x.

Van Leeuwen, T., and W. Mulder, 2008, Velocity analysis based on data correlation: Geophysical Prospecting, **56**, 791–803, http://dx.doi.org/10.1111/j.1365-2478.2008.00704.x.

Virieux, J., and S. Operto, 2009, An overview of full waveform inversion in exploration geophysics: Geophysics, **74**, no. 6, WCC1–WCC26, http://dx.doi.org/10.1190/1.3238367.

Xu, S., D. Wang, F. Chen, G. Lambaré, and Y. Zhang, 2012, Inversion on reflected seismic wave: 82nd Annual International Meeting, SEG, Expanded Abstracts, http://dx.doi.org/10.1190/segam2012-1473.1.

Yang, T., and P. Sava, 2011, Wave-equation migration velocity analysis with time-shift imaging: Geophysical Prospecting, **59**, 635–650, http://dx.doi.org/10.1111/j.1365-2478.2011.00954.x.

DOI http://dx.doi.org/10.1190/segam2013-0897.1